REMARKS

The Office Action dated March 27, 2009 has been received and carefully noted. The above amendments and the following remarks are being submitted as a full and complete response thereto.

Claims 1-10 have been rejected. Claims 1 and 6 have been cancelled, claims 2, 3, 7 and 8 have been amended and new claim 11 has been added. Thus, claims 2-5 and 7-11 are pending in this application. Support for the amendments may be found in the specification as originally filed, in particular in FIG. 1 and in paragraphs [0024] and [0025]. Applicants submit that no new matter is added. Applicants respectfully request reconsideration and withdrawal of all rejections.

Specification

The Specification has been amended in order to bring it in compliance with 37 CFR 1.77(b). If any further modifications are necessary, the Examiner is invited to contact the Applicant's undersigned representative via the telephone number below.

Drawings

FIG. 1 has been updated to show the steps of ionizing the fullerene and irradiating the fullerene ionized from said ion gun to the surface of said sample to be analyzed, thereby removing a contaminant present on the surface of said sample to be analyzed and ion-etching the surface of said sample to be analyzed. Accordingly, the Applicant respectfully requests that the objection to the drawings be withdrawn.

Rejection Under 35 U.S.C. §102

Claims 6-10 are rejected under 35 U.S.C. §102(b) as being anticipated by Watson et al. (U.S. Patent Publication No. 2003/0080292, hereinafter "Watson"). Claim 6 has been canceled and claims 7 and 8 have been amended. The Applicant respectfully traverses these rejections, insofar as they apply to newly amended claim 7 and its dependents, because Watson fails to disclose each and every feature of newly amended independent claim 7.

Newly amended independent claim 7 discloses, amongst other features, an electron spectroscopy analytical apparatus that comprises an ion gun ionizing a fullerene and irradiating the fullerene ionized, and the apparatus ionizes the fullerene and irradiates the fullerene ionized from said ion gun to the surface of said sample to be analyzed before irradiating the high-energy particle to said sample to be analyzed.

Watson discloses a "System and Method for Depth Profiling" (title). Watson does not, however, discuss an apparatus that includes an ion gun ionizing a fullerene, much less the ion gun ionizing a fullerene, as claimed. In fact, the specification of Watson does not even mention the word "fullerene." Although the Examiner implicitly acknowledges this, the Examiner construes the entire portion of the claim following the phrase "for ionizing and irradiating the fullerene" as a functional limitation which is not limiting subject matter. Claim 7 has been amended to include an ion gun ionizing a fullerene as structural, and therefore, limiting subject matter.

For at least the above reasons, Applicants respectfully submit that Watson does not anticipate newly amended independent claim 7 and claims 8, 9, 10 and 11, which depend therefrom. Therefore, claim 7 and claims 8, 9, 10 and 11 are allowable. Accordingly, Applicants respectfully request reconsideration and withdrawal of the 35 U.S.C. §102(b) rejections over Watson.

Rejection Under 35 U.S.C. §103

Claims 1-5 are rejected under 35 U.S.C. §103(a) as being unpatentable over Watson et al. (U.S. Patent Publication No. 2003/0080292, hereinafter "Watson") in view of Hill et al. (GB No. 2386747 A, hereinafter "Hill"). Claim 1 has been cancelled and claims 2 and 3 have been amended. The Applicant respectfully traverses this rejection because Watson and Hill, either independently or in combination, fail to disclose each and every feature at least of independent claim 2 nor are the features of independent claim 2 obvious in view of the references.

For example, independent claim 2 recites, amongst other features, an electron spectroscopy analysis method, wherein the method comprises steps of irradiating a high-energy particle to a sample to be analyzed under a vacuum atmosphere, and detecting a number and a kinetic energy of electrons emitted from said sample to be analyzed on the basis of a photoelectric effect, wherein the method comprises steps of ionizing a fullerene, irradiating the fullerene ionized to the surface of said sample to be analyzed before irradiating the high-energy particle to said sample to be analyzed, and etching the surface of said sample to be analyzed. The Applicant respectfully submits

that the alleged combination of Watson and Hill does not teach at least the electron spectroscopy analysis method as claimed.

The Examiner admits that Watson fails to disclose ionizing a fullerene and using a fullerene in an electron spectroscopy analysis method. However, the Examiner attempts to make up for this deficiency of Watson by using the ion source of Hill. Hill does disclose a "fullerene ion gun" (title) for "use as a probe in static time-of-flight secondary ion mass spectroscopy." However, Hill concerns a mass spectroscopy technique while Watson concerns an electron spectroscopy technique. These techniques are not related and are used for very different methods of analysis for entirely different purposes. The mere fact that the prior art may be modified in a manner suggested by the Examiner does not make the modification obvious unless there is a rational reason for the modification. *KSR Int'l Co. v. Teleflex Inc.*, 127 S.Ct. 1727 (2007). To facilitate review this analysis should be made explicit. *KSR Int'l Co. v. Teleflex Inc.*, 127 S.Ct. 1727 (2007). Here the Examiner's modification of Watson, even if it were possible, would be based on impermissible hindsight because the Examiner provides no rational reason to use fullerenes in the sputtering process of Watson, nor would such a use be recognized by one of ordinary skill in the art.

Further, there is no indication in Hill that "fullerene ion gun" is used in the electron spectroscopy analysis of Watson, or that it would even be possible to do so. Rather, Hill teaches that the fullerene ion gun is advantageous only for static time-of-flight secondary ion mass spectroscopy, not in an electron spectroscopy analysis method, as disclosed by Watson or as claimed. Static time-of-flight secondary ion mass

spectroscopy involves the analysis of material based on its mass and has no relation with any electron spectroscopy method or apparatus, much less the claimed electron spectroscopy method or apparatus. In fact, there is no mention of electron spectroscopy in Hill, nor is there any indication in Hill that the fullerene gun is capable of being used in conjunction with an electron spectroscopy method or apparatus.

Watson discloses that Auger electron spectroscopy (AES) measures a spectrum of the Auger electron that emitted from a surface of the sample by irradiating the sample with an electron beam. Hill discloses that Secondary Ion Mass Spectroscopy (SIMS) measures a mass of secondary ions emitted from the surface of a sample by making a primary ion incident upon the sample. Therefore, the two methods measure entirely different phenomena.

Hill uses C60 to gain "large intact molecules" from the sample. In the instant invention, a sputtered object of electron spectroscopic analysis should be both large and intact, but also should have relatively low surface damage after the ion is continuously irradiated.

As shown in the attached reference (F. Kollmer, Applied Surface Science, 231-232 (2004), p. 153-158), ion yield of "Irganox 1010" is around 1/1000 when C60 is used as the sputtering species (see Figure 3 and the Results and Discussion Section on page 156). This implies that SIMS with C60 as the sputtering species is not useful for observing 999/1000 cases.

It is well known that large molecules can be detected easily by using cluster ions from at least the following reference: Wittmaack, Surface Science, 90, (1979), p. 557 (hereinafter "Wittmaack"). However, there is no report correlating accurate detection of large molecules while keeping the damage to the sample surface relatively low in Wittmack or in the cited art.

Enhancement of molecule ion intensity by time of flight SIMS (TOF-SIMS) has been reported previously. Ion species are not limited to cluster ions, but also include O_2 and Cs etc. However, low surface damage **is not reported** for these sputtering ions, as in the instant invention. Indeed there would be little point to the claimed sputtering and analysis if it yielded the relatively high level of surface damage in most TOF-SIMS experiments. Reports of SIMS using C60 before 2003 discuss the amount of fragmented ions when only a very small amount of ions are irradiated.

Currently, specific properties of sputtering on C60 is discussed in academic journals and at academic conferences (see, e.g., Winograd, Analytical Chemistry, 2005, 143A (2005)). However, the sputtering methods require knowledge of X-ray Photoelectron Spectroscopy (XPS) and as well as knowledge of sputtering guns. Ion energy irradiated by a gas cluster ion beam, for example, varies if the amount of atoms varies. Particularly large irradiation devices, for example, are needed to provide a sufficient amount of atoms since retaining a gas cluster of less than 100 atoms is difficult. Further, it is also difficult for a gas cluster to reduce a pressure in an analytic device to 10^{-4} Pa or below. In comparison, fullerenes, such as C60, can relatively easily reduce the pressure in the analytic device to these pressures. In addition, with

fullerenes such as C60, control of both the etching and the energy level is relatively easily accomplished since the mass of the fullerenes remains constant. Therefore, it is especially advantageous to use fullerenes on samples with easily damaged surfaces.

In addition, the Applicants respectfully dispute the Examiner's contention that the proposed combination of Hill and Watson would be obvious. As described above, Watson and Hill are used for entirely different analytical techniques. Moreover, there is no suggestion, in either reference or elsewhere, that they should be combined. Therefore, the Applicants respectfully submit that it would not be obvious to combine the references in the manner suggested by the Examiner.

For at least the above reasons, Applicants respectfully submit that claims 1-5 are not obvious over the proposed combination of Watson and Hill. Thus, Applicants respectfully request reconsideration and withdrawal of the rejection of claims 1-5 under 35 U.S.C. §103(a) over Watson in view of Hill.

CONCLUSION

Applicants respectfully submit that this application is in condition for allowance and such action is earnestly solicited. If the Examiner believes that anything further is desirable in order to place this application in even better condition for allowance, the Examiner is invited to contact Applicants' undersigned representative at the telephone number listed below to schedule a personal or telephone interview to discuss any remaining issues.

In the event that this paper is not being timely filed, Applicants respectfully petition for an appropriate extension of time. Any fees for such an extension, together with any additional fees that may be due with respect to this paper, may be charged to Counsel's Deposit Account Number 01-2300, referencing Docket Number 029567-00008.

Respectfully submitted,

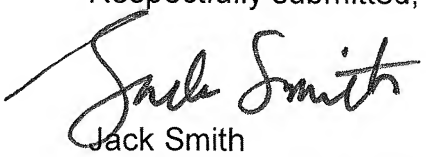

Jack Smith
Registration No. 61,986

Customer No. 004372
ARENT FOX LLP
1050 Connecticut Avenue, N.W.,
Suite 400
Washington, D.C. 20036-5339
Tel: (202) 857-6000
Fax: (202) 638-4810

JS/tnj

Surface Science 90 (1979) 557–563

SECONDARY-ION EMISSION FROM SILICON BOMBARDED WITH ATOMIC AND MOLECULAR NOBLE-GAS IONS

K. WITTMAACK *
IBM Thomas J. Watson Research Center, Yorktown Heights, New York 10598, USA

Received 11 December 1978

The emission of Si^+ from a clean silicon surface has been studied for bombardment with various atomic and molecular noble gas ions at energies between 1.5 and 30 keV. It was found that the degree of ionization of Si^+ depends strongly (~linearly) on the projectile energy but only weakly on the projectile mass. These results suggest that the degree of ionization is heavily affected by the (dynamic) perturbation of the bulk properties of the bombarded area which increases with increasing nuclear energy deposition.

1. Introduction

As documented by recent review articles [1,2], the present state of understanding of secondary ion emission from ion-bombarded solids must still be considered rudimentary. Most of the progress achieved in this field during the last few years has been stimulated by interest in the analytical capabilities of secondary ion mass spectrometry (SIMS). For example, an empirical formalism has been evaluated for the relative degree of ionization, α_r^+, of (positively charged) atoms emitted from oxygen-saturated surfaces [3]. In this high sensitivity "mode" of SIMS analysis α_r^+ does not depend (within experimental accuracy) on the energy [3,4], mass or species [3] of the primary ions. Thus, α_r is governed almost exclusively by chemical effects introduced by the controlled presence of oxygen in the sample.

In oxygen-free systems, on the other hand, α_r has been found to depend markedly on the primary ion energy [4,5]. This effect has not yet been explained theoretically [1,2]. Since previous experiments have been restricted to bombardment with non-mass-analyzed argon ions [4,5], it was decided to extend earlier studies by using various mass-analyzed noble gas ions for bombardment over an energy range as large as possible. Also, bombardment with molecular ions was considered important since this allows the damage density in the collision cascade to be increased at the same energy per projectile atom [6].

* On leave from Gesellschaft für Strahlen-und Umweltforschung mbH, D-8042 Neuherberg, FR Germany (present and permanent address).

2. Experimental

The measurements were performed in a multi-technique surface analytical system [7] in which the SIMS section is almost identical to the quadrupole-equipped ion microprobe described previously by the present author [8,9]. In addition, the new system includes a velocity filter (Wien filter) for primary ion analysis. This feature allows an extension of the accessible energy range of the primary ions by a factor of two by use of doubly charged ions. These ions could be produced with sufficient intensity by increasing the discharge voltage of the ion source [10] to ~100V. Efficient production of molecular noble gas ions, on the other hand, required very low discharge voltages and source pressures of ~1 Pa (~10^{-2} Torr) [11]. The base pressure in the differentially pumped target chamber was 3×10^{-7} Pa (2×10^{-9} Torr). Except for the case of molecular noble gas ion production, the total chamber pressure did not exceed 10^{-6} Pa during bombardment.

Secondary ion intensities were recorded only after prolonged sputter cleaning with raster-scanned, focussed beams of relatively high current (0.1–1 μA, depending upon the ion energy). The cleanliness of the sample was checked by monitoring the intensities of SiO^+ and $SiOH^+$. After sputter cleaning, the intensities measured with a static, focussed beam (spot size $\lesssim$ 100 μm) were below 1 count/s for SiO^+ and below 10 counts/s for $SiOH^+$ at a beam current of 0.1 μA. Accordingly, Si^+ yield enhancement due to oxygen incorporation [1,12] can be neglected.

3. Results and discussion

Fig. 1 shows the projectile-energy dependence of the Si^+ intensity, $I(Si^+)$, for normal beam incidence ($\theta = 0°$) on a sputter cleaned silicon sample. The results plotted in fig. 1 represent the intensities measured at the peak of the secondary ion energy distribution (see fig. 3). To avoid complications in data presentation due to the use of doubly charged primary ions (> 15 keV), $I(Si^+)$ is normalised to the number of incoming primary ions (PI). 10^{11} PI correspond to 16 nC (32 nC) of singly (doubly) charged ions.

As expected from previous measurements [4,5], $I(Si^+)$ increases with increasing projectile energy. Somewhat surprisingly, however, the abrupt increase observed [4,5] for argon bombardment above ~4 keV is not found with the other noble gas ions. On the basis of the data for Ne, Kr and Xe, one would have expected $I(Si^+, Ar)$ to increase above 4 keV as indicated by the dashed line in fig. 1. Above 10 keV, $I(Si^+, Ar)$ exceeds this interpolated intensity by about a factor of five. It can be shown that this marked enhancement is due to very effective 2p-excitation of Si via asymmetric Ar–Si collisions [13]. 2p-holes in Si can be produced also by Ne, Kr and Xe impact. In that case 2p-excitation is due to symmetric collisions between energetic Si recoils and other Si target atoms [13]. Compared to Ar–Si collisions,

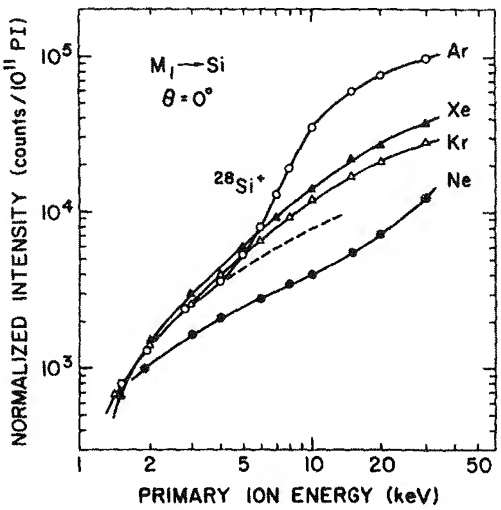

Fig. 1. Projectile-energy dependence of the intensity of Si^+ emitted from a clean silicon sample bombarded with various noble gas ions at normal incidence. The secondary ion intensity (counts) is normalised to the number of incoming primary ions (PI).

however, symmetric collisions, initiated by normally incident noble gas ions, are about a factor of 20 less effective in producing Si 2p-holes within the escape depth of sputtered atoms. Therefore, Auger deexcitation of excited Si *atoms* in vacuum contributes only very little ($\leqslant$10%) to the production of singly charged Si ions under Ne ($\leqslant$15 keV), Kr and Xe impact. Asymmetric Ne-Si collisions seem to become effective in producing Si 2p-holes at energies above 15 keV (cf. fig. 1).

Even without yield enhancement due to excess Si 2p-excitation (as in the case of Ar), the increase in Si^+ intensity observed with increasing primary ion energy E_0 is remarkable (fig. 1). If we assume that the energy distribution of sputtered particles (mostly neutrals) depends only slightly on the projectile energy, the average sputtering yield Y may be used to define the degree of ionization $\alpha^+ = \beta I(Si^+)/Y$. The constant β contains experimental parameters such as spectrometer transmission and the detector efficiency. Measured sputtering yields for Ar and Xe bombardment were taken from a recent study [14]. Data for Ne and Kr impact were interpolated using well-established formulas [15]. It was found that α^+ is largely independent of the projectile species (except for the Ar effect above ~4 keV). To demonstrate this result, the respective data for the lightest and the heaviest projectiles, Ne and Xe, are depicted in fig. 2.

At low energies the relative degree of ionization, $\alpha^+/\beta = I(Si^+)/Y$, is roughly proportional to E_0. Extrapolation to below 1 keV shows that α^+ approaches zero at very low impact energies. Above ~7 keV one observes slight deviations from a linear projectile-energy dependence and a small projectile-mass effect (fig. 2). Comparison with energy-deposition calculations [16] suggest that the *variation of* α^+ *is*

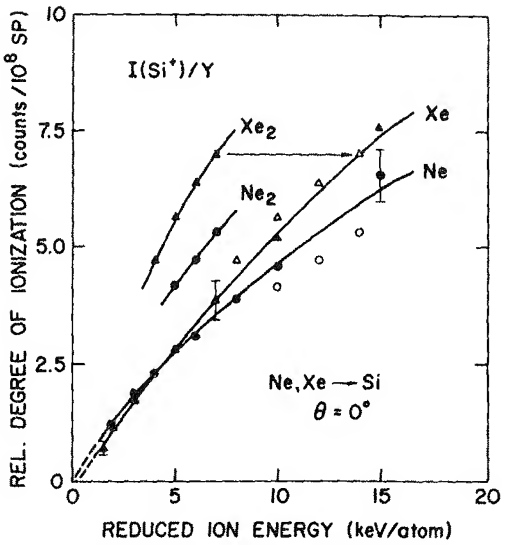

Fig. 2. Relative degree of ionization of Si^+ versus reduced primary ion energy (full circles and triangles). The open circles and triangles represent the data for Ne_2^+ and Xe_2^+ bombardment when plotted as a function of the energy per molecule (SP = sputtered particles).

related to the amount of energy deposited into damage, i.e. nuclear rather than electronic excitation determines the degree of ionization of an atom emitted from a clean solid. (The electronic energy loss is proportional to the projectile *velocity*.) This new idea is strongly supported by experiments with molecular noble gas ions. We have found that for dimer bombardment the intensity $I(M_1)_2$, normalized to the number of incoming projectile *atoms*, is larger by up to a factor of 2.5 than for monomer bombardment. The enhancement for doubly charged silicon ions, on the other hand, amounted to 30% at the most. A compilation of experimentally observed intensity ratios $I(M_1)_2/I(M_1)$ is given in table 1.

Since Si^{2+} emission is due to electronic excitation (2p-hole formation) any enhancement in Si^{2+} intensity must be attributed to an increase in sputtering yield. Comparison with sputtering yield ratios reported for dimer and monomer bombardment of silicon [6] support this interpretation. Accordingly, relative degrees of ionization for Si^+-emission due to dimer bombardment, $\alpha_2^+/\beta = I(M_1)_2/Y(M_1)_2$, can be evaluated using Si^{2+} intensity ratios for determining the respective sputtering yields $Y(M_1)_2$.

Results thus obtained for Ne_2^+ and Xe_2^+ bombardment are plotted in fig. 2 as a function of the reduced energy (keV/atom). Comparison with the data for bombardment with atomic ions indicates that the degree of ionization increases significantly if two projectile atoms arrive at the surface simultaneously (as a molecule) rather than separately (as two independent ions). Interpretation of this effect in terms of energy deposited into damage is supported by the fact that α^+ becomes

independent of the primary ion mass if the results are plotted as a function of the (total) primary ion energy (keV) instead of the reduced ion energy (keV/atom). The shifted data points are represented by open circles and triangles, respectively (fig. 2).

The significance of the (total) primary ion energy in secondary ion emission is also reflected by the secondary ion energy distributions. We have found that the shape of the energy spectrum depends upon the projectile energy (fig. 3). Related effects have been reported by other groups for low energy bombardment (<3 keV) [17]. Comparison of the energy spectra for Xe^+ and Xe_2^+ bombardment at 10 keV reveals a very close similarity (fig. 3). It should be noted that semilogarithmic plots of energy spectra as in fig. 3 exaggerate the effect of the projectile energy on the total secondary ion intensity. Taking into account the projectile-energy dependence of the secondary ion energy spectra would increase (!) the slope of curves such as in fig. 2 but not change the main conclusions.

On the basis of the present results, current models of secondary ion emission from clean surfaces [1,2] have to be revised. We have argued elsewhere already [1] that use of the band structures of unperturbed solids for the interpretation of deexcitation and neutralization phenomena occurring at ion bombarded surfaces is unjustified, in particular if heavy projectiles are involved. The (absolute) degree of ionization in the present experiments can be estimated [1] to be as low as $10^{-5} \lesssim \alpha^+ \lesssim 10^{-3}$, depending upon the primary ion energy. Accordingly, secondary ion emission from a clean silicon surface is a rare event which seems to take place only under certain favourable conditions. Since the energy *density* in a collision cascade increases with *decreasing* projectile energy [18,19], interpretation of the observed projectile-energy dependence in terms of ionization in high-temperature spikes is not possible. Alternatively we suspect that the yield enhancement is due to a diminution of the neutralization probability. It is conceivable that the departing ion, formed by some unknown process, experiences a reduced probability for neu-

Table 1
Secondary ion intensity ratios $I(M_1)_2/I(M_1)$ for bombardment of silicon with either monomer (M_1) or dimer $(M_1)_2$ noble gas ions; $I(M_1)$ and $I(M_1)_2$ are normalised to the number of incoming projectile atoms; the data represent intensity ratios measured at the respective peak of the secondary ion energy distributions (estimated accuracy ± 0.1)

Secondary ion	Projectile energy (keV/atom)	$I(M_1)_2/I(M_1)$			
		Ne	Ar	Kr	Xe
Si^+	5	1.5	1.7	2.3	2.5
Si^{2+}		1.0	1.0	1.1	1.3
Si^+	7	1.5	1.3 [a]	1.8	2.2
Si^{2+}		1.0	0.9	1.0	1.2

[a] Relative low ratio due to Ar-effect on ionization probability (see text).

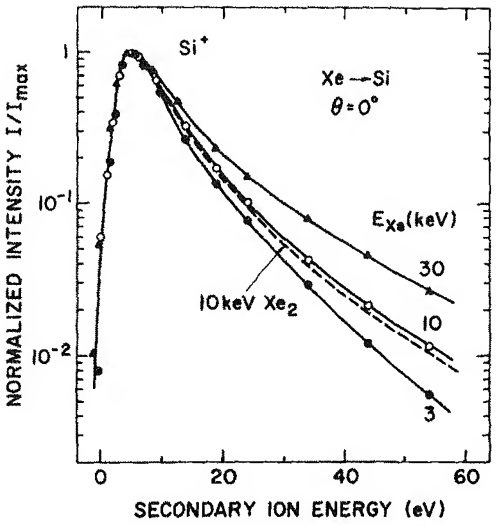

Fig. 3. Energy spectra of Si^+ (uncorrected) for Xe impact at normal incidence. Parameter is the xenon energy. The dashed line represents the secondary ion energy distribution for bombardment with 10 keV Xe_2^+.

tralization as the nuclear excitation of the solid increases; in other words, a necessary condition for a relatively high degree of ionization is that the bulk features are destroyed locally during ion emission, i.e. during the lifetime of the collision cascade (dynamic randomization). If this picture is correct the lateral extension as well as the time constant of the collision cascade would be important. The possible significance of these parameters deserves further investigation.

4. Conclusion

This study has shown that the degree of ionization of singly charged silicon ions emitted from a clean solid depends strongly on the projectile energy. Taking into account the fact that the absolute degree of ionization is very small, the results suggest that (in the absence of a chemical enhancement effect) sputtered particles are emitted as (singly charged) ions only if the damage created in the individual cascade is large at the very point of emission. Accordingly, the degree of ionization will become extremely low at impact energies below 1 keV because sputtering events involving heavy perturbation become very rare.

References

[1] K. Wittmaack, in: Inelastic Ion–Surface Collisions, Eds. N.H. Tolk, J.C. Tully, W. Heiland and C.W. White (Academic Press, New York, 1977) p. 153.

[2] G. Blaise, in: Material Characterization Using Ion Beams, Eds. J.P. Thomas and A. Cachard (Plenum, New York, 1978) p. 143.
[3] A.E. Morgan and H.W. Werner, Anal. Chem. 48 (1976) 699, ibid, 48 (1977) 927.
[4] J. Maul and K. Wittmaack, Surface Sci. 47 (1975) 358.
[5] K. Wittmaack, Surface Sci. 53 (1975) 626.
[6] H.H. Andersen and H.L. Bay, Radiation Effects 19 (1973) 138, J. Appl. Phys. 45 (1974) 953.
[7] M.A. Frisch, W. Reuter and K. Wittmaack in: Proc. 13th Ann. Conf. Microbeam Analysis Society, Ann Arbor (1978) p. 8.
[8] K. Wittmaack, Rev. Sci. Instrum. 47 (1976) 157.
[9] K. Wittmaack, in: Advances in Mass Spectrometry, Vol. 7A, Ed. N.R. Daly (Heyden, London, 1978) p. 758.
[10] K. Wittmaack and W. Wach, Nucl. Instr. Methods 143 (1977) 7.
[11] K. Wittmaack, J. Vacuum Sci. Technol. 16 (1979).
[12] K. Wittmaack, Surface Sci. 68 (1978) 118.
[13] K. Wittmaack, Surface Sci. 85 (1979) 69.
[14] P. Blank and K. Wittmaack, J. Appl. Phys. 50 (1979) 1519.
[15] P. Sigmund, Phys. Rev. 184 (1969) 383.
[16] D.K. Brice, J. Appl. Phys. 46 (1975) 3385.
[17] A.R. Krauss and D.M. Gruen, Nucl. Instr. Methods 149 (1978) 547.
[18] P. Sigmund, Appl. Phys. Letters 25 (1974) 169.
[19] D.A. Thompson, R.S. Walker and J.A. Davies, Radiation Effects 32 (1977) 135.
[20] G. Blaise, Radiation Effects 18 (1973) 235.

The Magic of cluster SIMS

Low topography, enhanced high-mass ion yields, and low damage cross sections have researchers thinking about new applications that may lead to the discovery of new biology.

Nicholas Winograd
Pennsylvania State University

Every once in a while, a breakthrough propels a mature field into new dimensions—just as the discoveries of MALDI and ESI opened MS to biologists and, incidentally, racked up Nobel Prizes for their inventors. This sort of metamorphosis is currently under way in bioimaging because of the remarkable properties of cluster ion beam sources being used with secondary ion MS (SIMS).

These sources direct a beam of energetic ions (typically several thousand electron volts) at the target; the ions initiate a cascade of moving particles, causing desorption of secondary molecular ions. The two most significant features of this approach are that desorbed molecules arise specifically from the top portion of the sample, making it useful for surface analysis, and that the primary ion beam can be focused to a submicrometer-sized spot where, in conjunction with TOF detection, images of the surface can be obtained.

Because mass spectral information is associated with each pixel, molecule-specific pictures can be acquired. This article will review the "magical" properties of cluster ion sources for SIMS experiments and consider the scope of new applications, particularly in bioimaging.

TOF-SIMS and the expanding world of MS

The desorption of molecules induced by ion bombardment was first observed >30 years ago. This technique was one of the earliest schemes for detecting organic molecules that were not amenable to electron impact ionization, which, at that time, was the only option for this type of analysis (*1*). The approach has some fundamental flaws, however, and has been eclipsed by MALDI and ESI in recent years. The major weakness is that the bombardment process causes a lot of damage to the sample surface. If the dose is too high (>~1% of the number of surface molecules), a carbon residue from molecular fragmentation builds up on the surface and the signal disappears. This 1% restriction, the so-called static limit, obviously puts a damper on detecting very small sample concentrations.

This problem was addressed during the 1980s by using fast atom bombardment and by dissolving the sample in a liquid matrix so that the surface could be continually regenerated (*2*). The very nature of the desorption process, however, still leads to complicated spectra, congested by matrix and fragment ions created during the impact of the primary particle with the target. Moreover, the mass range is limited to fairly small molecules with a molecular weight less than several thousand daltons. With MALDI or ESI, not only do the spectra consist primarily of molecular ions without fragments, but it is feasible to detect ions with a mass range extending to millions of daltons, thereby opening up the assay to peptides, proteins, and DNA (*3*, *4*). Imaging with MALDI has also been demonstrated, although the effective lateral resolution is, so far, limited to tens of micrometers.

With these difficulties, why is SIMS still being pursued as a viable option for MS measurements? The answer is surface sensitivity and submicrometer imaging capability. In addition, no matrix is required—samples can be studied in "as-received" condition. SIMS is one of the best ways to characterize organic thin films, polymer surfaces, semiconductor surfaces, and a host of other related materials (*5*). In many cases, the lateral resolution is in the 100-nm range. With SIMS, it may be possible to examine patterned surfaces, various arrays, and even single biological cells, all with the molecular specificity unique to MS. Hence, researchers have been willing to put up with mass spectra of less than stellar quality as a trade-off for access to a unique class of samples.

Many of these restrictions are changing with the introduction of primary ion beam sources composed of molecular clusters rather than single atomic particles. These sources greatly simplify SIMS spectra and exhibit an extended mass range for desorbed molecules. Accumulated damage appears to be much less of an issue, and in some cases it is possible to exceed the static limit, thereby increasing sensitivity. Cluster sources with imaging capability are just now entering the marketplace. There is a sense that the field is indeed poised for one of those unusual jumps in performance that can open new vistas.

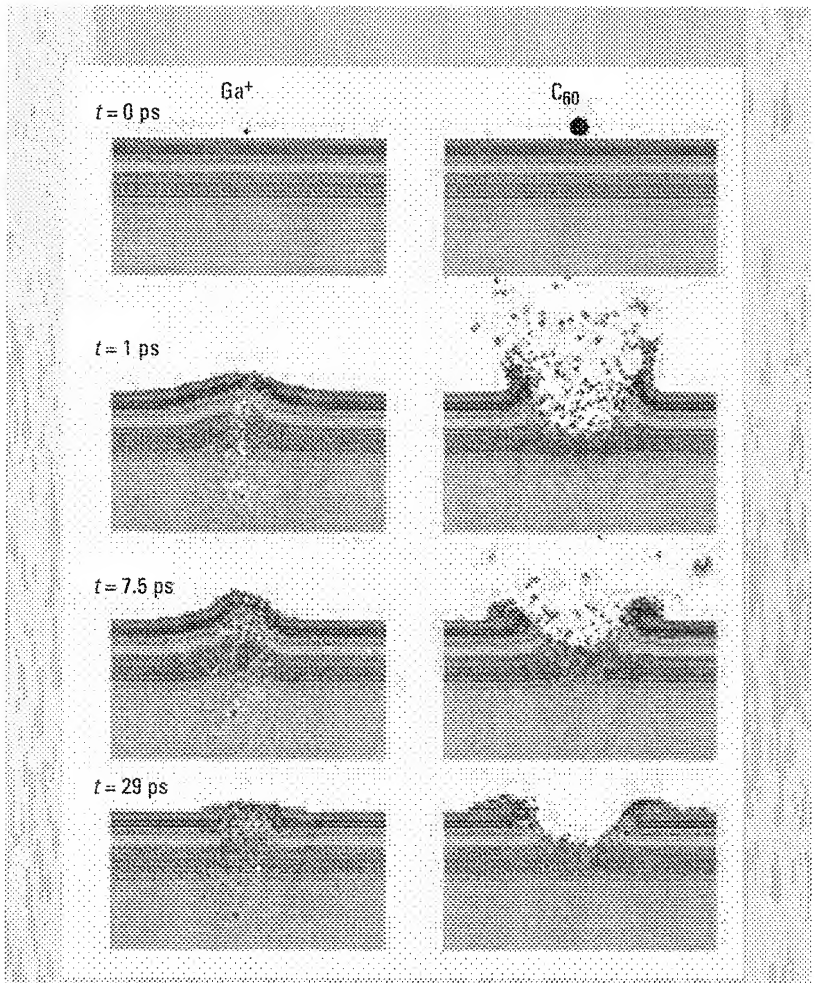

FIGURE 1. Impacted silver.

Snapshots from a molecular dynamics computer simulation of 15-keV C_{60} and 15-keV Ga^+ bombardment of silver metal. The view is from the side of a portion of a $10 \times 10 \times 10$ nm^3 microcrystallite containing 612,000 atoms. Sputtered silver atoms induced by Ga^+ bombardment are not visible because they are ejected at an angle out of the slab. The layers are colored so that atomic displacements are more easily visible. (Adapted from Ref. 6.)

Cluster ion sources work their magic

Before the special effects associated with cluster bombardment are described, it is useful to have a picture of how desorption occurs during atomic bombardment. These pictures are created from molecular dynamics computer simulations of the ion-bombardment event (*6*). These types of calculations have been developed over many years and are available primarily for metallic targets, although a lot of recent effort has been devoted to the behavior of organic thin films. A typical trajectory of a 15-keV Ga^+ bombardment of a silver crystal surface is shown

in Figure 1. The time sequence shows that a considerable disruption occurs deep into the crystal and around the impact point. Very little material is removed from the solid, in part because the energy is deposited so far below the surface.

Clusters of atoms behave very differently. For example, consider bombarding the silver surface with a 15-keV C_{60} buckminsterfullerene, instead of Ga^+. In this case, each carbon atom in this cluster would have a kinetic energy (KE) of 15,000/60 or 250 eV. This energy is much greater than the C–C bond strength in C_{60} of ~5 eV, so one might expect that the buckyball would be completely shattered upon impact. As a consequence, the solid might react as though 60 individual 250-eV carbon atoms hit it simultaneously, each creating its own cascade of moving atoms. The fact that the KE of 250 eV per atom in the cascade is much lower than the 15,000 eV associated with Ga^+ suggests that the deposited energy will remain closer to the surface, more effectively leading to desorption.

A computer simulation of a C_{60} impact on silver is shown in Figure 1. These are rather heroic calculations because they require modeling >600,000 silver atoms to contain the trajectory within the model microcrystallite. Notice the formation of a crater with mesoscopic dimensions. Nearly 400 atoms are sputtered per incident buckyball, a >15-fold increase over Ga^+ bombardment. Although the yield is much higher, the depth of damage is smaller than for the corresponding atomic bombardment, extending only a few layers below the bottom of the crater. These simulations show that a nonlinear enhancement of the yield of silver occurs, which means that the yield from the 15-keV C_{60} bombardment is >60× the yield from 250-eV carbon bombardment. Finally, note that the time of the trajectory is considerably longer for cluster bombardment—29 ps for C_{60} versus 3 ps for gallium. These pictures clearly suggest that when clusters are used, the energy deposition process is quite different than when atomic beams are used.

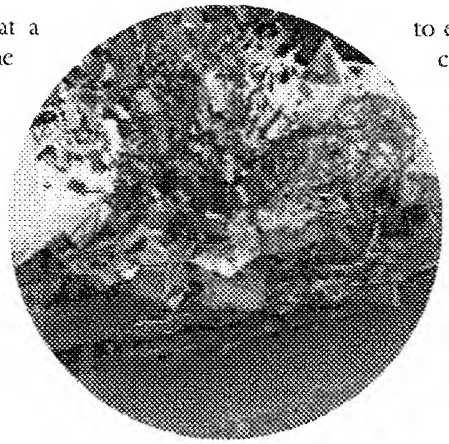

Characterizing **complex multilayer** structures is of **increasing importance,** particularly **to the electronics** industry.

Au_3 and C_{60} projectiles

The fact that cluster ion sources are more effective at desorbing molecules was discovered more than 15 years ago (*7*, *8*). The projectiles SF_6 and Cs_xI_y enabled the acquisition of SIMS spectra with enhanced sensitivity for many polymer and organic thin films. The SF_6 source was quickly improved and commercialized. Other species, such as aromatic hydrocarbons, massive glycerol clusters, and various inorganic complex ions, were also found to be effective. Although the SIMS community conceded that these sources could significantly improve the quality of data, only a few laboratories aggressively pursued applications. Perhaps the reason for this lapse is that the sources themselves are not conducive to everyday use. Maintenance issues, low beam current, and/or lack of focusing have relegated most of these guns to the back of the drawer.

The emergence of Au_3 and C_{60} ion sources has resolved many of these issues and has stimulated a major new push to map all the benefits of cluster ions. The Au_3 source utilizes a liquid-metal ion gun (LMIG; *9*, *10*). For traditional SIMS experiments, the LMIG consists of a field emitter tip normally coated with gallium (the choice of projectile for Figure 1). Gallium ions are extracted from the tip and refocused into the sample with a spot size of <50 nm. The ion KE needs to be fairly high to achieve this spot size. Typically, values of 15–40 keV are required.

It is possible to use gold as the coating metal. Early designs had short lifetimes due to the high temperature required to force the gold to coat the emitter tip. It was soon discovered that AuGe or AuSi eutectic alloys could be used at much lower temperatures. Because there is more than one component, the source emits a variety of ions, which necessitates using a mass filter. Even with these issues, a significant intensity of Au_3 can still be used for SIMS experiments. The source exhibits a very high brightness, has a lifetime >500 h, and can be focused to a spot size of ~200 nm. This source has become very popular, and most instruments have already been retrofitted to accept it.

The C_{60} source has a more conventional design. A stable vapor pressure for C_{60} can be created by heating the source to ~300 °C. The vapor can then be very efficiently ionized by conventional electron impact (*11*). When high-quality focusing optics have been used, spot sizes of ~2 μm have been obtained, and designs are being discussed for 200-nm operation. This source is robust, exhibits a lifetime of >500 h before cleaning, and has plenty of beam current for SIMS experiments.

These two species appear to have complementary properties. Both ions enhance high-mass ion yields by factors of 100,000 or more. The damage accumulation rate appears to be higher with Au_3 than with C_{60} (*11*), which might be expected because the KE of each gold atom is greater than the KE of each carbon atom. Currently, the focusing properties of the gold source are better than those of the C_{60} source, so imaging experiments are more practical with the LMIG design. In any case, both of these projectiles are yielding new applications in a variety of fields.

Implications for depth profiling

Characterizing complex multilayer structures is of increasing importance, particularly to the electronics industry. When ion beams are used, it is possible to systematically remove material from the sample in a layer-by-layer fashion and subsequently determine the composition of each layer by MS. For atomic ion

sources, variation in yield due to crystallographic effects and beam-induced mixing of the layers limits the best achievable depth resolution. This effect can be minimized in various ways, such as using low ion energy and sample rotation. Although these strategies are successful, they add to the complexity of the measurements.

The computer simulation graphics shown in Figure 1 suggest that the use of projectiles such as C_{60} might allow better depth resolution without the need to resort to such trickery. For example, the fact that very little subsurface damage occurs relative to the atomic bombardment shows that the layers are peeled away in a more uniform fashion. Moreover, because the size of the buckyball is greater than the lattice constant of a typical metal substrate, crystallographic effects where sputtering yields depend upon the nature of the surface structure might not be so serious.

Recent experiments that compared the use of C_{60} and Ga^+ sources in the analysis of NiCr multilayers bear out this hypothesis (*12*). A direct bombardment with 15-keV C_{60} produced a crater bottom with a root-mean-square roughness of 2.5 nm versus 100 nm for atomic bombardment. The resulting depth resolution was as good as the best value reported using sample rotation and low-energy bombardment. This consequence is particularly important because higher-energy beams are required if depth-profiling measurements are combined with imaging experiments. So, Magical Property #1 is that the topographical roughening that is normally encountered during erosion experiments seems to be absent when a large cluster such as C_{60} is used.

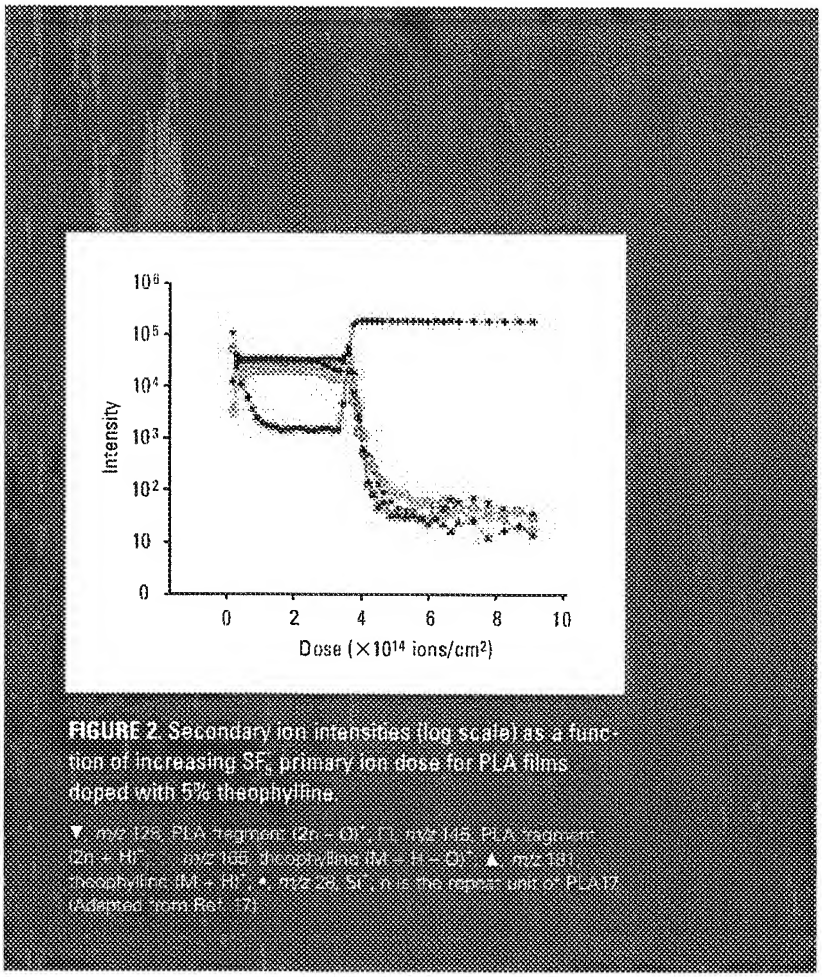

FIGURE 2. Secondary ion intensities (log scale) as a function of increasing SF₅ primary ion dose for PLA films doped with 5% theophylline.

▼, m/z 129, PLA fragment; ◆, m/z 145, PLA fragment; ▲, m/z 181, theophylline (M + H)⁺; ●, m/z 29, SF₅⁺. (Reproduced from Ref. 17.)

Enhancement of molecular ion yields

Although the advantages of cluster ion sources for observing higher-molecular-weight molecules have been touted for some time, the true significance of the effect has only recently been brought into clear focus by Vickerman and colleagues (*13*, *14*). They showed that the secondary ion yields of molecular ions in the 1000–3000-Da range induced by cluster bombardment are enhanced by at least 300-fold over corresponding atomic bombardment experiments. For several samples, including the small peptide gramicidin D, the molecular ion could only be observed when the cluster source was used. This type of result has been obtained for many classes of organic and inorganic samples. Much-improved SIMS spectra are seen from polymer surfaces such as polystyrene and polyethylene terephthalate. The yields and desorption efficiencies of C_{60} and Au_3 have been compared in detail. In general, the ion yield enhancements are about the same for both projectiles, but the desorption efficiency (yield divided by the damage cross section) is significantly higher for C_{60}.

The reasons behind this enhancement effect are not yet clear. The computer simulations clearly show that the yield of neutral atoms is higher, and that a propensity exists for bigger sputtered clusters to form. Until calculations are available for molecular solids, however, these types of pictures will not be available for things such as peptides. A few experiments have been performed to compare the amount of material removed with an atomic source and a cluster source. In one case, Langmuir–Blodgett techniques were used to prepare a multilayer structure of known thickness, and the number of incident particles required to remove all the layers was measured (*15*). For molecular weights <~500 Da, the enhancement effect can be largely explained by an increase in the yield of neutral molecules, presumably because of the unusual nature of the collision cascade (Figure 1).

For larger molecules, such experiments have not been possible, and it seems unlikely that the enormous dramatic effects seen by the Vickerman group can be explained solely on the basis of enhanced sputtering. Perhaps the nature of the plume that is formed as the molecules take off is ideally suited to ionization. Perhaps other, unknown mechanisms are at work. This will clearly be an interesting project for future research. So, Magical Property #2 of cluster ion beams, particularly C_{60}, is that the usable mass range for SIMS experiments is considerably extended and that the sensitivity for high-mass ions is greatly improved. However, except for a few pathological cases, molecules heavier than 10,000 Da cannot be desorbed intact. The mass range of MALDI and ESI-MS is still much larger than that of cluster SIMS.

Molecular depth profiling

Another surprise is in store. Typically, the sensitivity of SIMS measurements is limited by the eventual accumulation of damage on the surface of a bombarded solid. This damage is caused either by direct fragmentation of surface molecules by the primary

ion or by displaced lattice atoms just below the surface. Frequently, if an organic film is bombarded long enough, a graphitic overlayer eventually coats it, and all the molecular information is lost. Depth profiling in a fashion analogous to that reported for the NiCr stack discussed earlier has simply not been possible with molecular films. However, for cluster ion beams, the amount of damage accumulation is significantly lower than for atomic projectiles (*16*). The secondary ion formation efficiency is increased even more than the secondary ion yield itself.

This point has been dramatically demonstrated by Gillen et al., who recently reported that the SIMS spectra of small drug molecules doped into a polymer matrix consisting of polylactic acid (PLA) remain stable under SF_5^+ cluster ion bombardment (*17*). Very little damage accumulated during the experiment. The result of a typical depth profile for a 5% concentration of theophylline doped into PLA is shown in Figure 2. These particular results are important for examining molecular concentration gradients in polymer films used in drug delivery applications. Molecular stability of this sort has also been observed for histamine dissolved into a water–ice matrix (*18*). Unfortunately, not every molecular solid behaves so nicely, but if the experiments can be generalized, they will have major implications for the analysis of complex multilayer structures.

The reasons behind these observations are still under investigation. One thought is that the enhanced yield associated with cluster bombardment is effective at removing any accumulating chemical damage. For PLA, for example, the polymer unzips during bombardment, resulting in an unusually large sputtering yield. Similarly, for a water–ice matrix, ~2500 water molecules are desorbed for each C_{60} impact, presumably enough to sweep away any chemical fragments left on the surface from a previous impact. Although this explanation is certainly reasonable, the hypothesis will need to be proven so that the conditions for molecular depth profiling can be appropriately optimized.

Implications for chemical imaging

Imaging with TOF-SIMS is usually performed by a pulsed, focused ion beam scanned across the sample. A TOF mass spectrum is recorded at every point in the image. If special software is used, it is possible to construct an image that displays ion intensity versus position for any mass or set of masses. Depending on the type of beam, the lateral resolution ranges from 50 nm to several micrometers. Although this method is potentially a powerful and unique approach to imaging, it has a fundamental flaw. As the pixel size approaches submicrometer dimensions, the number of molecules available for analysis becomes vanishingly small. For example, there are only 40,000 molecules per layer in a 100-nm spot, corresponding to 6×10^{-20} mol. Given the restrictions of static SIMS, only a few hundred of these molecules would be amenable to analysis. This issue has prevented the technology from reaching its full potential.

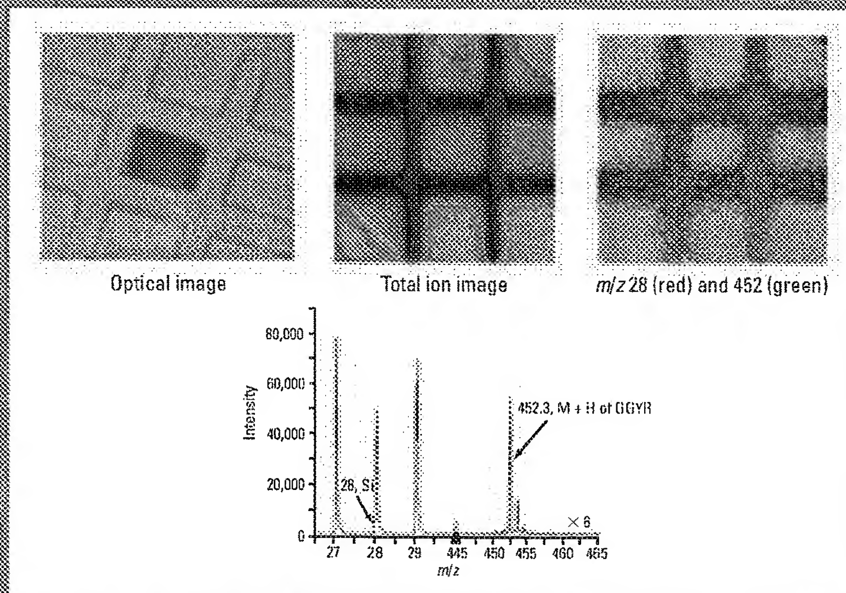

FIGURE 3. Tic-tac-toe.

A 300-nm film of Gly-Gly-Tyr-Arg (GGYR) in an [illegible] matrix. The central square has been etched to 150 nm. The change in [illegible] the optical image is caused by [illegible] interference effects. The field of view is [illegible] μm. The spectrum shown corresponds to the total ion image.

At this point, it should be clear where we are heading with cluster SIMS. Because desorption yields and efficiencies are greatly enhanced, there should be a direct benefit to chemical imaging experiments. In Figure 3, a tetrapeptide (Gly–Gly–Tyr–Arg) has been dissolved into the sugar trehalose at the 1% level (*19*). Trehalose is an interesting matrix because peptides retain their folded configuration in a glassy film; the sputtering yield of trehalose under C_{60} bombardment is large enough to allow molecular ion signals to be retained under high-bombardment dose conditions. A 300-nm-thick pad of the peptide on silicon was etched with C_{60} to a 150-nm film thickness. An image of the sample was then acquired where the intensity of the molecular ion at *m/z* 452.3 and the silicon mass at *m/z* 28 were monitored. The resulting image exhibits very high contrast, with as many as 30 counts in each pixel. Such contrast is only possible because the static limit can be

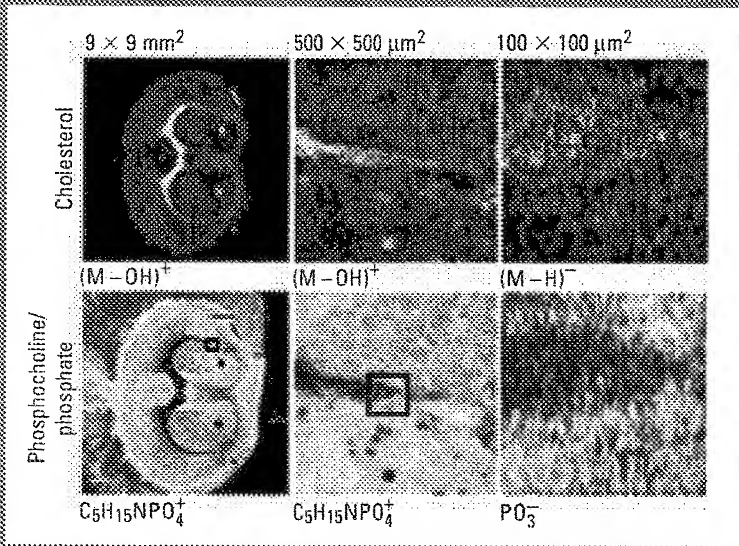

FIGURE 4. Mouse brain images.

[illegible]

exceeded with retention of an intense peptide molecular ion signal. It is technically easy to record these images for various amounts of peptide removed and thus create a 3-D molecular map. So far, only systems that exhibit a very high sputtering yield are amenable to this type of analysis, and each sample needs to be examined on a case-by-case basis. Nonetheless, it is easy to think about many potential applications, including those involving assay of peptide arrays, interlayer mixing in multilayer organic structures, and combinatorial chemistry (*20*).

Bioimaging of tissue and single cells

Perhaps the most far-reaching application of TOF-SIMS imaging with cluster ion beams is the determination of the lateral distribution of specific substances in biological tissue and cells. MS is a unique approach to this problem, because labeling is not required and the spectra have high molecular specificity. Several studies that use Au_3^+ bombardment to determine the lipid distribution in freeze-dried mouse brain have illustrated the power of this approach (*21*, *22*). Molecular ion peaks from cholesterol, sulfatides, phosphatidylinositols, and phosphatidylcholines were all identified in a mass spectral image from several areas of various sizes (Figure 4). Several previous studies have used atomic ion and massive cluster ion bombardment to report on the distribution of the phospholipid headgroup fragment at *m/z* 184 (*16*). However, the mouse brain studies are the first to report that a broad repertoire of ions up to 1000 Da were measured. The availability of these cluster ion sources opens many new possibilities for more of these studies.

Other enormous implications include the ability to examine biological processes on a molecular level and to assess the effects of therapeutic drug treatments on individual cells. Several labs have achieved single-cell bioimaging with atomic primary projectiles (*23–25*). Although the images have been plagued by low signal from the diverse array of membrane molecules, lipid rearrangements at highly curved membrane junctions have been followed. If these types of experiments could be extended to molecules other than phosphatidylcholine fragments and elemental species, much more biochemical information could be acquired. However, SIMS analysis with atomic projectiles is restricted to the section of the cell exposed to the vacuum interface; in other words, examining the vertical molecular distribution of single cells and 3-D imaging is not possible.

The magical properties of cluster SIMS address both of these conundrums. Cluster ion projectiles greatly increase the secondary ion yield, particularly of high-mass fragments and molecular ions. This ability increases not only the mass range of biomolecules amenable to study but also the number of molecules per image pixel. Brighter pixels result in better contrast between adjacent pixels, leading to a more complete and informative chemical map of a single cell. This attribute of C_{60} is nicely depicted by comparing the molecule-specific images taken with an indium atomic primary source and a C_{60} cluster source of a *Spirostomum* cell (Figure 5). *Spirostomum* is a protozoan well known for its ability to contract to one-quarter of its length on a millisecond timescale and for its use in acute toxicity testing. Its large size makes it a particularly attractive cell system for preliminary C_{60} image experiments where the lateral resolution is not as high as that of atomic probes. A quick comparison of the two images establishes that cluster SIMS produces better-quality images than atomic SIMS. The spectra that correspond with these images show that the phosphocholine signal is enhanced ~300-fold with C_{60} versus indium.

In addition to the advantages of enhanced ion yield and improved imaging, C_{60} should be able to depth profile through a cell. Preliminary results from our lab show that the lipid signal remains localized to a freeze-fractured paramecium after C_{60} bombardment. This prospect is tantalizing because cells can be controllably sectioned and molecularly imaged without chemically damaging the molecules of interest or altering their native distribution in the cell. In a Harry Potter-crazed world, everyone needs a little magic, and in the single-cell SIMS community, that magic lies in cluster projectiles.

Down the road

The properties of cluster SIMS—low topography, enhanced high-mass ion yields, low damage cross sections with molecular

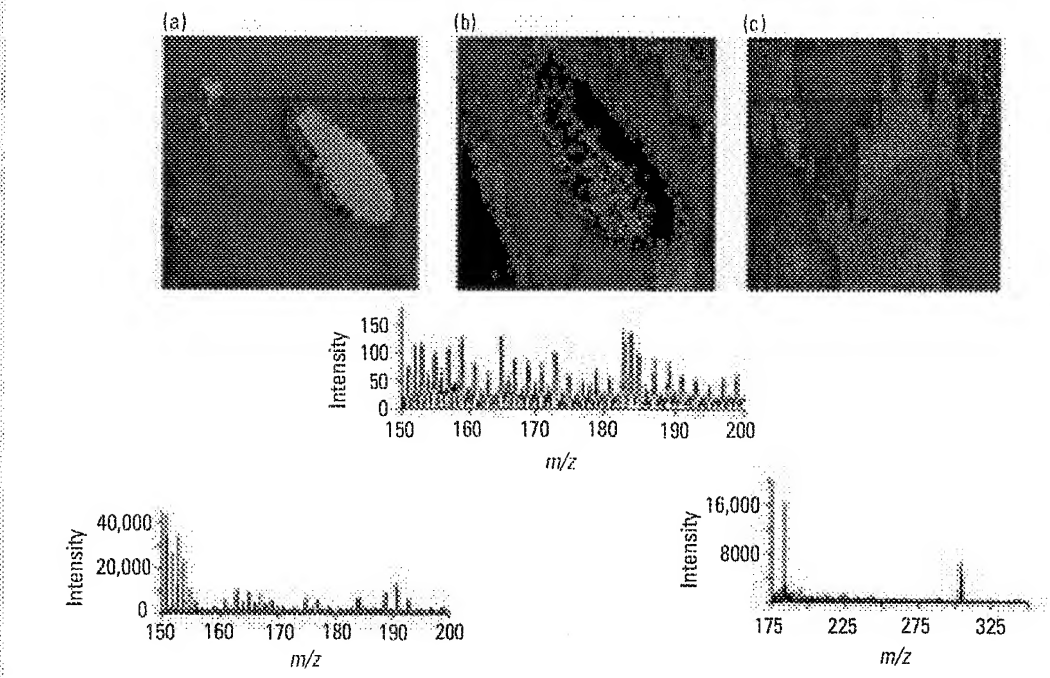

FIGURE 5. SIMS images of freeze-dried *Spirostomum* taken with different primary ion sources.

(a) C_{60} probe image and mass spectrum; 700 × 700 μm² field of view. (b) In-probe image and mass spectrum of (a) in 380 × 380 μm² field of view. A 300-fold signal increase in *m/z* 184 (phosphocholine) is observed with the C_{60} primary projectile. (c) C_{60} probe image and mass spectrum of freeze-dried *Spirostomum* that was incubated in 0.1 mM cocaine (*m/z* 304); 400 × 400 μm² field of view. Rapid warming during sample preparation resulted in sublimation of the intracellular material and altered the distribution of cocaine.

depth profiling—are stimulating researchers to think about new applications. As these tools become more commonly available, we anticipate that the unique nature of this methodology will inevitably lead to the discovery of new biology—the specific location of small molecules will be pinpointed with exquisite detail in single cells. Experiments with molecular depth profiling also offer new analysis paradigms for multilayer organic thin films and other complicated structures important to nanotechnology. We are still at an early stage of development in fully realizing the magical properties of cluster SIMS, and not every system behaves as expected. Nonetheless, the guidelines are in place to establish a unique form of 3-D molecular analysis.

Sara Ostrowski and Juan Cheng provided unpublished data for this manuscript and helped invaluably in developing the ideas presented. Funding from the National Science Foundation and the National Institutes of Health is also gratefully acknowledged.

Nicholas Winograd is a professor at Pennsylvania State University. His research interests focus on ion/solid interactions and bioimaging. Address correspondence about this article to him at 209 Chemistry Bldg., Penn State University, University Park, PA 16802 (nxw@psu.edu).

References

(1) Benninghoven, A.; Jaspers, D.; Sichtermann, W. *Appl. Phys.* **1976**, *11*, 35–39.
(2) Barber, M.; et al. *Nature* **1981**, *293*, 270–275.
(3) Karas, M.; Hillenkamp, F. *Anal. Chem.* **1988**, *60*, 2299–2301.
(4) Fenn, J. B.; et al. *Science* **1989**, *246*, 64–71.
(5) Benninghoven, A. *Appl. Surf. Sci.* **2003**, *203*, 1–2.
(6) Postawa, Z.; et al. *J. Phys. Chem. B* **2004**, *108*, 7831–7838.
(7) Blain, M. G.; et al. *Phys. Rev. Lett.* **1989**, *63*, 1625–1628.
(8) Appelhans, A. D.; Delmore, J. E. *Anal. Chem.* **1989**, *61*, 1087–1093.
(9) Davies, N.; et al. *Appl. Surf. Sci.* **2003**, *203*, 223–227.
(10) Kersting, R.; et al. In *Secondary Ion Mass Spectrometry, SIMS XII*, Proceedings of the International Conference on Secondary Ion Mass Spectrometry, Brussels, Belgium, Sept 5–10, 1999; Benninghoven, A., et al., Eds.; Elsevier: Amsterdam, 2000; pp 825–828.
(11) Weibel, D.; et al. *Anal. Chem.* **2003**, *75*, 1754–1764.
(12) Sun, S.; et al. *Appl. Phys. Lett.* **2004**, *84*, 5177–5179.
(13) Wong, S. C. C.; et al. *Appl. Surf. Sci.* **2003**, *203*, 219–222.
(14) Weibel, D. E.; Lockyer, N.; Vickerman, J. C. *Appl. Surf. Sci.* **2004**, *231–232*, 146–152.
(15) Sostarecz, A. G.; et al. *Appl. Surf. Sci.* **2004**, *231–232*, 179–182.
(16) McMahon, J. M.; Dookeran, N. N.; Todd, P. J. *J. Am. Soc. Mass Spectrom.* **1995**, *6*, 1047–1058.
(17) Mahoney, C. M.; Roberson, S., V.; Gillen, G. *Anal. Chem.* **2004**, *76*, 3199–3207.
(18) Wucher, A.; et al. *Appl. Surf. Sci.* **2004**, *231–232*, 68–71.
(19) Cheng, J.; Winograd, N. *Anal. Chem.*, submitted.
(20) Xu, J.; et al. *J. Am. Chem. Soc.* **2004**, *126*, 3902–3909.
(21) Touboul, D.; et al. *Anal. Chem.* **2004**, *76*, 1550–1559.
(22) Sjoevall, P.; Lausmaa, J.; Johansson, B. *Anal. Chem.* **2004**, *76*, 4271–4278.
(23) Colliver, T. L.; et al. *Anal. Chem.* **1997**, *69*, 2225–2231.
(24) Ostrowski, S. G.; et al. *Science* **2004**, *305*, 71–74.
(25) Cliff, B.; et al. *Rapid Commun. Mass Spectrom.* **2003**, *17*, 2163–2167.

Available online at www.sciencedirect.com
SCIENCE DIRECT®
ELSEVIER
Applied Surface Science 231–232 (2004) 153–158
applied surface science
www.elsevier.com/locate/apsusc

Cluster primary ion bombardment of organic materials

F. Kollmer*
ION-TOF GmbH, Gievenbecker Weg 15, D-48149 Münster, Germany

Available online 25 May 2004

Abstract

In order to evaluate their potential for molecular surface analysis, we applied monoatomic (Ga, Cs, Au, Bi) as well as polyatomic (SF_5, Au_n, Bi_n, C_{60}) primary ions to a series of organic samples. For the model system Irganox 1010 on LDPE we determined the secondary ion yield, the disappearance cross section and the resulting ion formation efficiency as a function of the primary ion energy. As a general result the efficiency is improved with the mass of the monoatomic primary ion. A further increase is obtained by the use of polyatomic primary ions. According to this, highest efficiencies are obtained for C_{60}, the lowest for Ga. Additionally, molecular imaging was performed on real world samples (electronic components, pharmaceuticals): for this a cluster LMIS operated with Ga, AuGe or Bi was applied. The results reveal the potential of cluster SIMS to overcome existing limitations and to establish TOF-SIMS for new applications in the fields of polymers, biology and medicine.

Keywords: Cluster SIMS; Molecular imaging; Efficiency; Pharmaceuticals; Salbutamol

1. Introduction

The analysis of organic solid surfaces has been improved over the years by the static SIMS approach [1]. In spite of all the advances in this field, there are still many challenges in tapping the full potential of molecular SIMS. In particular, molecular imaging requires the most sensitive measurement conditions since the number of available molecules is very limited.

One approach to increase the sensitivity is the application of laser postionization [2,3]. However, ionization probabilities for molecules are often low and the appropriate postionization parameters must be applied to minimize photon induced fragmentation. Therefore postionization seems to be no general solution for molecular surface analysis.

A more successful approach to increase the sensitivity for the analysis of organic surfaces is the use of polyatomic primary ions. In 1987, Appelhans et al. [4] applied a neutral SF_6^0 beam to avoid charging effects on non-conducting polymer surfaces. The unexpected result of these experiments was a gain in secondary ion yield of several orders of magnitude compared to atomic primary ions of equivalent energy. Retrospectively, these investigations must be seen as the advent of "cluster SIMS".

In the following years several groups continued to investigate the application of molecular primary ions, and it has been demonstrated that the secondary ion yields of most organic compounds can be enhanced by several orders of magnitude [5–9]. Concerning the analysis of organic surfaces, the corresponding increase in the ion formation efficiency E is even more important since E is a measure for the sensitivity of the entire analysis process (see below) [10].

* Tel.: +49-251-1622-311; fax: +49-251-1622-199.
E-mail address: felix.kollmer@ion-tof.com (F. Kollmer).

0169-4332/$ – see front matter
doi:10.1016/j.apsusc.2004.03.101

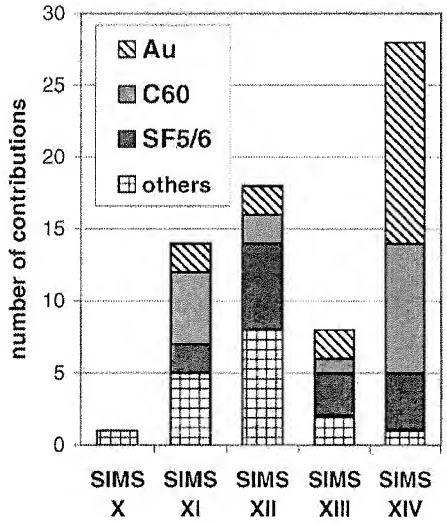

Fig. 1. Number of contributions applying different primary ion beams at previous SIMS conferences.

Au cluster ions produced by a liquid metal ion source (LMIS) were applied for the first time by Benguerba et al. in 1991 [11]. In this systematic investigation, the secondary ion yield of different Au_n clusters ($n = 1-5$) was compared as a function of cluster size and energy per atom. For organic surfaces like phenylalanine a strong, non-linear increase with the number of constituents in the cluster was reported. The outstanding imaging capabilities of an Au cluster LMIS were first demonstrated at the SIMS XII conference [12,13]. In these investigations, the yield enhancement obtained with Au_1 and Au_2 over Ga was necessary to determine the lateral distribution of organic contaminants and additives on different surfaces.

Although the fundamental advantages of polyatomic primary ion bombardment were well-known, they were slowly introduced to the SIMS community. Fig. 1 reflects the increasing application of polyatomic primary ions in recent years. Especially the currently growing importance of C_{60} and Au cluster primary ions becomes obvious.

2. Terms and definitions

In order to compare the capabilities of different primary ions species the following definitions are useful [10].

The secondary ion yield $Y(X_i^q)$ is defined as the number of detected secondary ions $N(X_i^q)$ divided by the total number N_{PI} of applied primary ions:

$$Y(X_i^q) = \frac{N(X_i^q)}{N_{PI}}$$

The index i distinguishes between the different emission channels and q the charge of the secondary particle X_i.

As a result of the primary ion impact, the surface coverage of a certain molecule is reduced by desorption or fragmentation. Provided the ionization probability is constant, the signal intensity of a certain species X_i^q decays exponentially according to

$$N(X_i^q) = N(X_i^q)_{t=0} \exp(-\sigma(X_i^q)\mathrm{PIDD}),$$

where PIDD is the number of primary ions per analyzed area. The damage cross section $\sigma(X_i^q)$ is given by the slope of the exponential decay and corresponds to the mean area from which no further ion X_i^q can be generated after a primary ion impact.

An important quantity is the secondary ion formation efficiency E which is defined as the secondary ion yield per disappearance cross section:

$$E(X_i^q) = \frac{Y(X_i^q)}{\sigma(X_i^q)}$$

The efficiency E corresponds to the number of detected secondary ions X_i^q if the uppermost monolayer of the analyzed surface is completely sputtered. Therefore E is a cumulative measure of the sensitivity of the analysis process.

In the case of organic surfaces, the achievable lateral resolution is often not limited by the spot size of the primary ion beam, but by the number of ions which can be generated from a given area. Hence the efficiency E not only determines the achievable detection limits in surface spectrometry but also limits the useful lateral resolution Δl via:

$$\Delta l = \left(\frac{N}{E}\right)^{1/2}$$

where N is the number of secondary ions detected from the area Δl^2 if the uppermost monolayer of this area is completely consumed.

3. Experimental

All experiments were carried out using a TOF-SIMS IV instrument. The instrument is equipped with a 25 kV LMIS operated with either Ga, AuGe or Bi. Since a large variety of Au and Bi clusters is emitted, two pulsing units are utilized to separate different primary ion species by their time-of-flight (mass gate). Furthermore, the instrument is equipped with a 10 kV electron impact source operated with C_{60}. In this case, a dynamic 90° deflection unit allows the separation of a single primary ion species (*q*/*m* ratio) from the primary ion beam.

The lateral resolution and pulse width performance achieved for different primary ions is given in Table 1. Relative cluster currents of Bi and Au are shown in Fig. 2. For an easier comparison the current of the singly charged monomers Au_1^+ and Bi_1^+ is normalized to 100%. Compared to Au, Bi emits bigger clusters and produces higher cluster currents. The current for the singly charged trimer is about a factor of five higher for bismuth. Moreover bismuth emits a variety of doubly charged clusters. These clusters are interesting since the kinetic energy of a cluster for a given source potential is doubled. Especially Bi_3^{++} provides intense cluster currents as well as a good beam performance (Table 1) which is supposed to be caused by the low energy spread of these species.

Table 1
Primary ion capabilities

	Ga_1^+	Au_1^+	Au_3^+	Bi_3^{++}	C_{60}^+	C_{60}^{++}
Mass (u)	69	197	591	627	720	720
Energy (keV)	25	25	25	50	10	20
Spot size (nm)	100	150	200	100	3000	3000
Pulse width (ns)	0.6	0.7	1.2	0.7	1.4	1.1

The lateral resolution Δl is obtained in the imaging mode; the pulse width is obtained in the spectroscopy mode.

In order to compare the capabilities of different primary ion species as well as different primary ion sources, a standard set of samples was prepared. The influence of the primary ion properties (species, number of constituents, energy) on the secondary ion formation was systematically studied on Irganox 1010. To ensure a (sub)monolayer preparation, the samples were prepared by spincoating Irganox 1010 onto LDPE (low density polyethylene).

In particular to compare the molecular imaging capabilities, a color filter array (CFA) was analyzed (Fig. 3). This sample is ideally suited for this purpose since its molecular surface is very homogenous, laterally structured and comparatively insensitive to electron bombardment. It consists of an array of three different kinds of colored squares (RGB pixel) with an area of ~5 μm × 5 μm each.

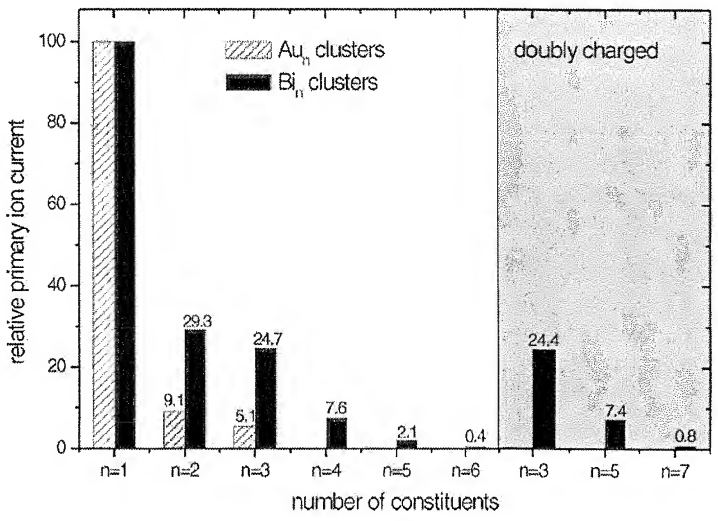

Fig. 2. Normalized primary ion currents for Au and Bi clusters as a function of cluster size and charge. Au_1^+ and Bi_1^+ currents are normalized to 100%.

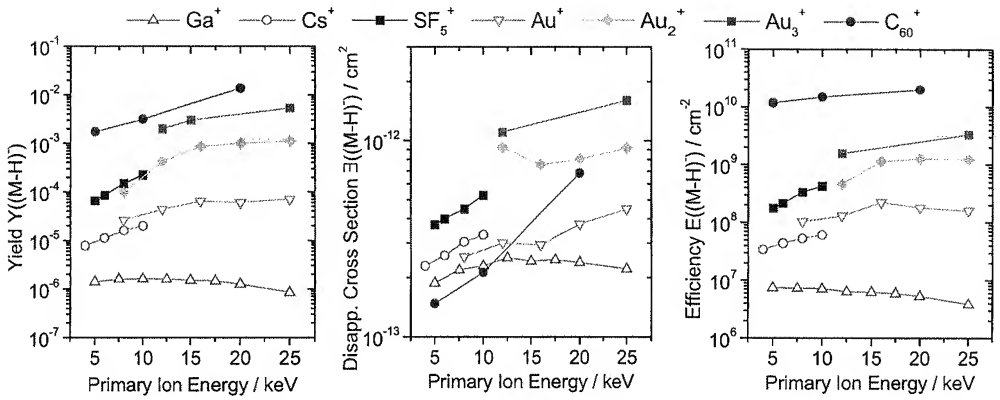

Fig. 3. SI yield Y, disappearance cross section σ and efficiency E of the Irganox 1010 quasi-molecular ion $(M-H)^-$ as a function of the PI energy and species.

As an example for the investigation of pharmaceuticals, the lateral distribution of salbutamol ($C_{13}H_{21}NO_3$, $m = 239$ u) was determined. Salbutamol is used as an asthma drug. In commercially available aerosol sprays it is placed on sugar beads. For the preparation, a single dose of the aerosol (Salbuhexal N®, Hexal AG, Germany) was sprayed onto a clean silicon wafer.

4. Results and discussion

4.1. Irganox 1010

In Fig. 3 the secondary ion yield Y, the disappearance cross section σ, and the resulting ion formation efficiency for the quasi-molecular ion $(M+H)^-$ of Irganox 1010 are shown for a variety of primary ion species as a function of their energy. In general, the yield increases with the primary ion mass as well as with the primary ion energy. Only for Ga^+ the yield decreases at higher energies after it reaches a maximum at about 10 keV.

Due to the higher primary ion mass, the yield is increased for Cs^+ as well as for Au^+ compared to Ga^+. A further non-linear increase is achieved when changing from atomic to polyatomic projectiles. The trend of the disappearance cross section σ is similar (except for C_{60}), but less pronounced. While the secondary ion yield is increased by more than three orders of magnitude between Ga^+ and $Au_3{}^+$, the disappearance cross section is increased by less than one order of magnitude. As a result the ion formation efficiency E is maximized for heavy polyatomic projectiles.

Our current understanding is that this is due to a very homogeneous and near surface energy transfer to the sample. The highest efficiency is achieved for C_{60} which offers the maximum number of constituents and the minimum energy per primary atom. Therefore, C_{60} deposits most of its energy very close to the sample surface [14]. This results in a "softer" desorption process and also in very low fragmentation spectra [15].

In this study, Bi primary ions were only applied to acquire positive TOF-SIMS spectra of Irganox 1010. Efficiency values obtained for the high mass fragment $C_{56}H_{83}O_9{}^+$ ($m = 899$ u) are comparable to the values for Au clusters. However, a significant efficiency gain of a factor of 3 is observed when changing from $Bi_3{}^+$ (25 keV) to $Bi_3{}^{++}$ (50 keV).

4.1.1. Color filter array

For imaging purposes both the efficiency and the corresponding useful lateral resolution Δl, as well as the spot size of the primary ion beam must be considered. Fig. 4 gives an example of the analysis of a real world sample. All images are acquired until the signal intensity drops to $1/e$ of the initial value, which corresponds to the same degree of sample consumption and can be considered as a direct measure for the efficiency.

Whereas the low efficiency of Ga^+ does not give a clear determination of the lateral distribution of the pigments, the distribution is clearly shown by using

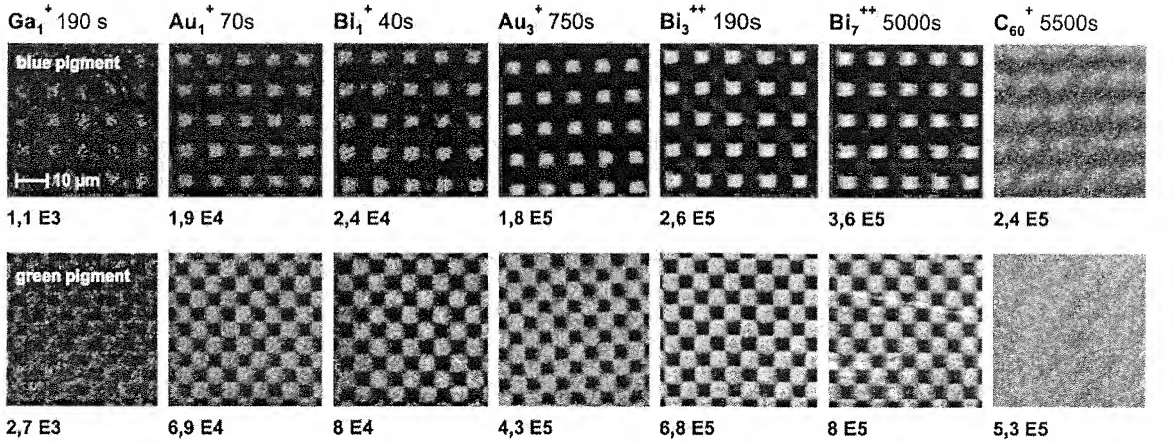

Fig. 4. Positive secondary ion images of blue (m = 413 u) and green (m = 641 u) pigments of a CFA (color filter array). Above each image the primary ion species and the measurement time is displayed. Underline: corresponding signal intensity. Primary ion source potential: metal clusters 25 kV, C_{60} 10 kV.

Au_1^+ as primary ion species. Also the measurement time is reduced due to the higher disappearance cross section of Au_1. The results for Bi_1^+ are similar to Au_1^+. The reduced measurement time is explained by easier mass filtering allowing longer primary ion pulses for Bi_1^+. A further distinct increase in efficiency is possible by the application of Au_3^+ and Bi_3^{++}. Here the higher cluster current (Fig. 2) and the higher energy of Bi_3^{++} leads to a much faster acquisition compared to Au_3^+. Bi_7^{++} offers the highest efficiency but the slight increase over Au_3^+/Bi_3^+ is obtained at the expense of a very long acquisition time.

The application of C_{60}^+ to this sample reveals some disadvantages concerning small area imaging. Due to the low brightness of the source, the primary ion current must be reduced to reach a spot size of about 3 µm. The reduced current results in a long measurement time and anyhow the lateral distribution of the pigments is only just perceptible (Fig. 3).

The efficiency obtained corresponds to a useful lateral resolution Δl of about 1300 nm for Ga^+, 400 nm for Au_1 and Bi_1 and about 150 nm for the cluster ions. These values can be considered as a lower limit for the reasonable spot size of the primary ion beam. In the case of Ga^+, the beam can easily be focused down to the 100 nm range which is useless because of the low efficiency. In the case of C_{60}, the situation is contrary. Whereas the efficiency would

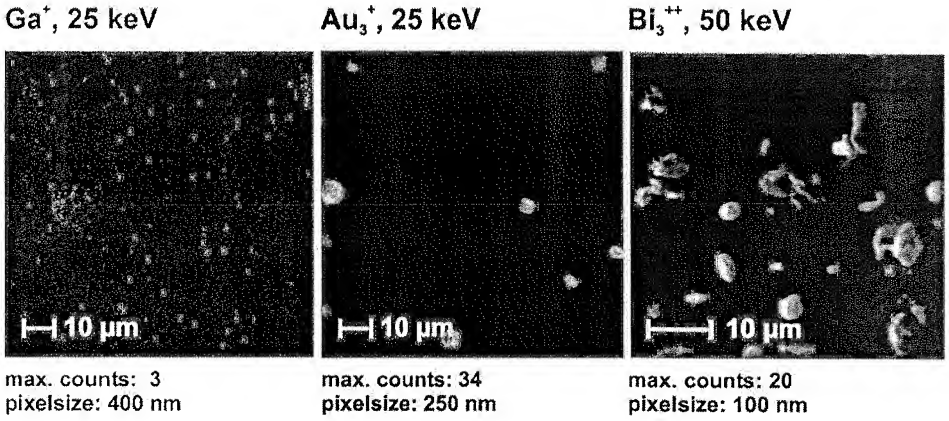

Fig. 5. Positive secondary ion images showing the lateral distribution of the quasi-molecular ion signal $(M + H)^+$ of salbutamol.

allow the use of a spot size in the 100 nm range, the achievable spot size is far from this.

Only in the case of the cluster ions emitted by the LMIS, the useful lateral resolution matches the spot size achieved.

4.2. Salbutamol

Fig. 5 shows another example for the outstanding capabilities of a state-of-the-art cluster LMIS. The lateral distribution of the asthma drug salbutamol cannot usefully be determined by the use of Ga, although the surface was completely consumed during the analysis. The application of Au_3^+ or Bi_3^{++} improves the analytical result, the higher efficiency allows a detailed determination of the lateral distribution of salbutamol. The substance can be identified even by analyzing the area of a single pixel which corresponds to the detection of about 2×10^{-20} mol of salbutamol from an area of 100 nm × 100 nm. This example emphasizes the potential of cluster SIMS to overcome existing boundaries and to establish TOF-SIMS for new applications.

5. Conclusion

It has been shown that for some samples cluster ion beams have the potential to increase the secondary ion yield by more than three orders of magnitude compared to Ga. Even the corresponding efficiency can be increased by more than two orders of magnitude. Whereas C_{60}^+ primary ions offer the highest sensitivity and the lowest fragmentation at least for the investigated samples, the large spot size of the ion beam hampers the analysis of small (sub-μm) areas.

Only liquid metal cluster ion sources provide the necessary brightness to combine high spatial resolution with high cluster currents. Moreover, the now established Au cluster LMIS combines these fundamental capabilities with practical advantages such as stability, lifetime, ease-of-use and the possibility of selecting between atomic and molecular primary ions. A promising alternative concerning cluster currents and performance can be a cluster LMIS operated with bismuth instead of Au.

Acknowledgements

I gratefully acknowledge the contributions of my colleagues of the ION-TOF company to this work. In particular I would like to thank R. Moellers, P. Hoerster, T. Grehl, H.-G. Cramer, D. Rading, E. Niehuis as well as R. Kersting and B. Hagenhoff of the TASCON company.

References

[1] A. Benninghoven, Surf. Sci. 299/300 (1994) 246.
[2] N. Winograd, Anal. Chem. 65 (14) (1993) 622A–629A.
[3] F. Kollmer, N. Bourdos, R. Kamischke, A. Benninghoven, Appl. Surf. Sci. 203–204 (2003) 238–243.
[4] A.D. Appelhans, J.E. Delmore, D.A. Dahl, Anal. Chem. 59 (13) (1987) 1685–1691.
[5] A.D. Appelhans, J.E. Delmore, Anal. Chem. 61 (10) (1989) 1086–1093.
[6] W. Szymczak, K. Wittmaack, Methods and Mechanisms for Producing Ions from Large Molecules, Plenum Press, New York, 1991, pp. 123–127.
[7] E.A. Schweikert, M.G. Blain, M.A. Park, E.F. da Silveira, Nucl. Instrum. Meth. B 50 (1990) 307.
[8] G. Gillen, S. Roberson, Rapid Commun. Mass Spectrom. 12 (1998) 1303.
[9] D. Stapel, M. Thieman, A. Benninghoven, Appl. Surf. Sci. 158 (2000) 362.
[10] F. Koetter, A. Benninghoven, Appl. Surf. Sci. 113 (1998) 47.
[11] M. Benguerba, A. Brunelle, S. Della-Negra, J. Depauw, H. Joret, Y. Le Beyec, M.G. Blain, E.A. Schweikert, G. Ben Assayag, P. Sudraud, Nucl. Instrum. Meth. B 62 (1991) 8–22.
[12] B. Hagenhoff, R. Kersting, D. Rading, S. Kayser, E. Niehuis, Proceedings of the SIMS XII, 1999, p. 833.
[13] R. Kersting, A.P. Pijpers, B. Hagenhoff, R. Verlaek, D. Stapel, A. Benninghoven, Proceedings of the SIMS XII, 1999, p. 825.
[14] D. Weibel, S. Wong, N. Lockyer, P. Blenkinsopp, R. Hill, J.C. Vickerman, Anal. Chem. 75 (2003) 1754–1764.
[15] R. Kersting, B. Hagenhoff, F. Kollmer, R. Möllers, E. Niehuis, Proceedings of the SIMS XIV, 2003.